Available online at www.sciencedirect.com
SCIENCE DIRECT®
ELSEVIER
Journal of Nuclear Materials 337–339 (2005) 1058–1063
journal of nuclear materials
www.elsevier.com/locate/jnucmat

Identification of molecular carbon sources in the JET divertor by means of emission spectroscopy

S. Brezinsek [a,*], A. Pospieszczyk [a], M.F. Stamp [b], A. Meigs [b], A. Kirschner [a], A. Huber [a], Ph. Mertens [a], JET-EFDA contributors [1]

[a] *Institut für Plasmaphysik, Forschungszentrum Jülich GmbH, EURATOM-Association, D-52425 Jülich, Trilateral Euregio Cluster, Germany*
[b] *Euratom/UKAEA Fusion Association, Culham Science Centre, Abingdon, Oxon OX14 3DB, UK*

Abstract

Strong light emission from the C_2 Swan band and the CD Gerö band has been observed during strike-point sweeps in the corner region of the inner MKII SRP divertor of JET. The light emission could be correlated to the decomposition of probably soft hydrocarbon layers at the corner entrance. The C_2/CD photon-flux ratio indicates a preferred emission of C_2 and thus of C_2D_y particles. The layer has been removed within one H-mode discharge, where the strike point was fixed at the corner. In the consecutive discharges no enhanced light emission from C_2 and CD could be observed and the C_2/CD photon-flux ratio drops significantly. The spectroscopic observations are in line with measurements on the quartz microbalance (QMB). A similar layer in the outer divertor could not be identified from the spectroscopy.

PACS: 52.70.Kz; 52.40.Hf; 52.25.Vy; 52.55.Fa; 33.20.Lg
Keywords: Spectroscopy; JET; Carbon impurities; Erosion and deposition; Divertor

1. Introduction

The first wall of JET is made of graphite composites and the impact of deuterium on these plasma-facing areas can cause chemical erosion [1]. The deposition of eroded material finally takes place in the form of hydrocarbon layers in the divertor. The analysis of tiles installed in the MKII GB configuration has shown that the major part of the layers is finally deposited on the horizontal target plate in the corner region of the inner divertor [2]. In contrast to the deposition-dominated inner divertor, the outer divertor is nearly balanced in erosion and deposition. The hydrocarbon layers can be identified as an intermediate storage of carbon and fuel and can act as secondary erosion sources, while the primary erosion sources are not located in the divertor itself but rather in the main chamber [3]. The transport of eroded carbon from the main chamber into the divertor takes place in several steps and, thus, in several deposition and re-erosion processes.

Emission spectroscopy provides access to several species (CD, C_2, ...) of the dissociation chain of the

* Corresponding author. Tel.: +49 2461 61 6611; fax: +49 2641 61 3331.
E-mail address: s.brezinsek@fz-juelich.de (S. Brezinsek).
[1] See annex of J. Pamela et al., Fusion Energy 2002 (19th Int. Conf., Lyon, 2002), IAEA, Vienna.

0022-3115/$ - see front matter © 2004 Elsevier B.V. All rights reserved.
doi:10.1016/j.jnucmat.2004.10.114

methane and ethane family which are both usually observed in tokamaks with graphite inventory. The observation of the CD Gerö band and of the C_2 Swan band gives useful information about the sources, their location and quantity and about the dissociation process itself [4–6].

We present spectroscopic measurements from the inner and outer MKII SRP divertor where the intensity of different hydrocarbon break-up products and their variation as functions of the strike-point position and the plasma parameters have been investigated.

2. Spectroscopic setup

The measurements were performed by means of two sets of spectrometer systems observing two toroidally adjacent sectors [6,7]. The first system is equipped with a fibre optic bundle which covers both the inner and outer divertor. The second system uses a direct image, which has a better efficiency, but covers only the outer divertor.

Two survey spectrometers, in the following labelled as KS3A [6] and KME (Echelle arrangement in cross-dispersion, $\Delta\lambda/\lambda \simeq 21000$, $\lambda = 375$–$675\,\text{nm}$), are used with the fibre-optics system and allow the simultaneous detection of the C_2 Swan band, the CD Gerö band as well as different CII, CIII and D transitions. KS3A simultaneously observes the whole inner (ch2) and outer divertor (ch1) by means of two wide-angle fibres (Fig. 1(a)), and, additionally, the region along the vertical target (vt) plates down to the corner of the inner (ch3) and outer divertor (ch4) by means of two narrow fibres.

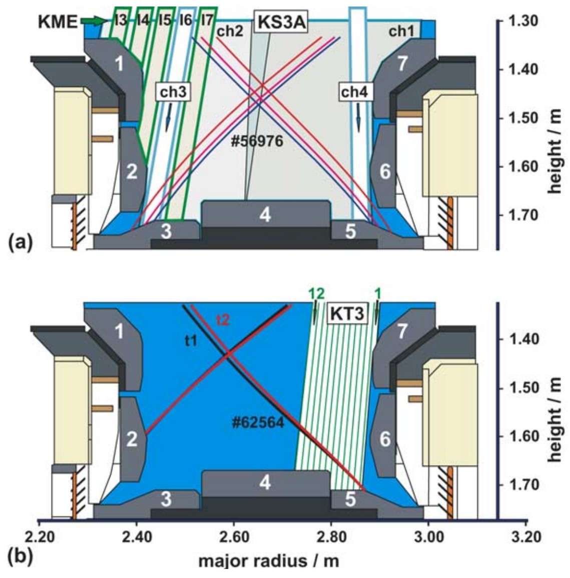

Fig. 1. The spectroscopic lines of sight in the JET divertor.

From shot to shot, one single fibre (I3–I7) from a set was used for KME. However, as Fig. 1 shows, the lines of sight are restricted at two locations in each divertor leg: (a) between the two vt plates and (b) in the corner.

Information about the released species in the outer divertor has been obtained by the second system which consists of two spectrometers labelled KT3A/B. They are in a direct line of sight and provide a good spectral resolution [7]. KT3A/B have been used for the detection of CD, C_2, CII and D. The observed range of 150 mm on the horizontal target (ht) is divided between 12 channels (Fig. 1(b)), and thus the spatial resolution is about 12.5 mm on plates 4 and 5. However, the view of the system is restricted at the corner entrance.

3. Experimental results and analysis

Plasma discharges with a sweep of the strike point (SP) have been performed to get local information about the carbon sources in the divertor. The SP and thus the point of highest ion flux is used as a tool to scan along the target plates and to analyse areas with different surface and impurity release properties like freshly deposited amorphous hydrocarbon (a-C:H) layers. The spectroscopic analysis of several discharges shows that the erosion and deposition of a-C:H layers in the corner region of the inner divertor seem to play a crucial role in the carbon transport towards the louvre. There is no indication from the spectroscopic analysis for the presence of similar types of layers in the corner region of the outer divertor.

3.1. Inner divertor

An SP sweep from target plate 2 to 3 and, thus, over the corner region was performed during the first part of discharge #56976 (L-mode, 1.5 MW ICRH). Fig. 2(a) shows two spectra which were recorded by means of KS3A (ch3) during the sweep. The first spectrum was measured at $t = 14.7\,\text{s}$, where the SP was directly positioned in the corner, and the second one at $t = 15.0\,\text{s}$, where the SP was already set on the ht plate (Fig. 2(b)). The second spectrum is representative of the inner divertor and of SP positions on the ht or vt plate, whereas the first one clearly shows additional features which were identified as the diagonal transitions ($\Delta v = 0, \pm 1, -2$) of the Swan band ($d^3\Pi \rightarrow a^3\Pi$) of C_2. The insert in Fig. 2(a) shows the time evolution of the C_2 photon flux (ϕ_{C_2}) taken from ch3 and ch2 of KS3A. The peak at 14.7 s is still visible in ch2, but the absolute value is reduced in comparison to ch3 due to averaging over the whole inner divertor span. The C_2 photon flux was integrated at the band head (515.2–516.7 nm). The maximum in ch3 shows the massive local increase of ϕ_{C_2} by more than a factor of five. The

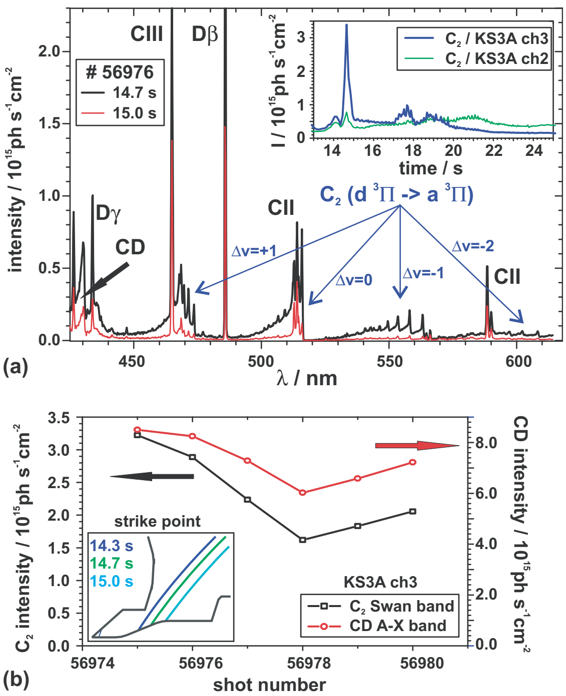

Fig. 2. (a) Two overview spectra showing strong light emission of the C_2 Swan band and the CD Gerö band. The SP is in the corner at $t = 14.7$ s. (b) Variation of ϕ_{C_2} and ϕ_{CD} in six discharges at $t = 14.7$ s.

maximum appears for about 400 ms, which corresponds to a radial SP shift of about 27 mm, and, thus, of about 75% of the radial extension of the ch3 view on plate 3 (35 mm). A deeper view into the corner is restricted and no information about light emission is available. However, we can conclude that the source is localised at the corner entrance and that the minimum extension is 27 mm in radial direction towards the corner.

A comparison between the spectra also shows a clear increase of the CD Gerö band ($A^2\Delta \rightarrow X^2\Pi$). The increase of the CD photon flux (ϕ_{CD}) in ch3 amounts to a factor of three in comparison with the reference at $t = 15.0$ s. This is significantly less than the increase of ϕ_{C_2}, but the simultaneous increase of CD and C_2 indicates the strong release of hydrocarbons and the presence of an a-C:H layer. Furthermore, the spectrum at $t = 14.7$ s shows no significant background from thermal radiation, thus the power density is not sufficient to heat up the layer above the detection limit for black body radiation for KS3A [8].

Pulse #56976 is the second one in a series of six consecutive plasma discharges (#56975–#56980) which have an identical phase at the beginning. This allows the study of the hydrocarbon release and the properties of the deposited a-C:H layer over several discharges. Fig. 2(b) shows the shot-to-shot variation of the peak value of the Swan and Gerö band emission measured at the same time in all discharges. Over the first four discharges, a significant decrease of ϕ_{C_2} of more than 50% and of about 30% of ϕ_{CD} was observed. This is interpreted as a reduction of the hydrocarbon source or as a change of the layer composition. However, for the last two discharges of the series a significant increase of the photon flux of both C_2 and CD occurs. Following the previous argument, this might be connected to the deposition of fresh a-C:H layers.

It should be noted that in the later phase of the discharge (15–24 s) different gases (#56975–77: CD_4, #56978–80: D_2) have been injected into the divertor from different locations, all away from the observation volume of ch3 [9]. The amount of injected deuterium in the second phase increases strongly from discharge #56978 on. Obviously, this has an influence on the measurements in the first phase from the fifth discharge on. However, this indicates that, apart from the SP position and the plasma parameters, additional parameters influence the release of hydrocarbons from a-C:H layers. The massive emission of C_2 and CD light described here cannot always be seen with this strength when the SP touches exactly this radial location.

Further studies have been made in a series of identical discharges (#61379–#61381) with L- (3 MW NBI) and H-mode phase (12 MW NBI) where the SP was fixed at the expected location of the a-C:H layer. In addition to KS3A (ch2), KME and QMB were deployed in order to obtain information about the release of hydrocarbons in the corner.

Strong emission of C_2, CD and CII light is observed in the first discharge. In the second discharge a strong reduction of the photon fluxes occurs: 35% for C_2, 15% for CD and 45% for CII (H-mode phase). ϕ_{C_2} and ϕ_{CII} remain constant in the third discharge whereas the ϕ_{CD} increases slightly. This behaviour can be interpreted as the almost complete removal of a (soft) a-C:H layer in the first discharge. The constant photon fluxes of the next two discharges then represent the erosion from the bulk material or from another type of a-C:H layer. The change of the hydrocarbon source is supported by the change in the C_2/CD photon-flux ratio, which varies from 0.46 to 0.33 and finally to 0.29 (Table 1, whole band). A change in the composition of the released species takes place – C_2D_y becomes less important. Thus, the history of previously performed discharges plays an important role, which is also indicated by deposition measurements with the QMB [10].

The QMB was activated for the NBI part (#61379–#61381) and supports the spectroscopic results. The QMB measured a massive carbon deposition with a rate of 5.4 nm/s in the first discharge. This deposition rate is about 27 times higher than for similar DOC-L discharges and 3.2 times higher than for discharges in

Table 1
Variation of different photon fluxes (KS3A) and of the deposition rate (QMB) for discharges #61379–81

Discharge	ϕ_{C_2} (10^{15} ph s^{-1} cm^{-2} sr^{-1})	ϕ_{CD} (10^{15} ph s^{-1} cm^{-2} sr^{-1})	ϕ_{CII} (10^{15} ph s^{-1} cm^{-2} sr^{-1})	ϕ_{C_2}/ϕ_{CD} (band head)	ϕ_{C_2}/ϕ_{CD} (full band)	Deposition (nm/s)
61379	2.95	7.96	32.97	0.37	0.46	5.4
61380	1.83	6.88	18.26	0.26	0.33	−0.7
61381	1.73	7.38	18.31	0.23	0.29	−0.6

ϕ_{C_2}/ϕ_{CD} is given for the band heads and recalculated for the complete electronic transitions. The recalculation is actually performed by means of a correction factor of 1.25 which takes the rovibrational population of CD (3500 K) and C_2 (4000 K) into consideration.

horizontal target configuration. A large part of the released hydrocarbons reaches the area of the QMB, which is located near the louvre. However, the QMB shows erosion in the two successive discharges whereas the spectroscopy still shows C_2 and CD light emission (Table 1). One has to take into account that spectroscopy measures the gross release of particles whereas the QMB measures the net deposition – which is the difference between material deposition and re-erosion – that occurs at the remote location of the QMB mainly by chemical erosion due to atomic hydrogen.

KME (I6) was used to determine the rovibrational population of the eroded hydrocarbons. The measured spectrum of the Swan band, recorded during 3.7 s of the 5.5 s long H-mode phase, is shown in Fig. 3(a) as well as a modelled spectrum with an assumed rotational temperature of about 4000 K. Both spectra are in a reasonable agreement, and the deduced population is typical of the JET divertor. The corresponding spectrum in the L-mode phase shows no significant difference in the population, but a C_2 intensity lower by a factor of two. A reduction of the C_2 intensity of more than 35% in the H-mode and of 25% in the L-mode phase was observed in the successive discharge. This underlines the results previously presented, but shows also that the efficiency for the release of hydrocarbons from layers is higher with larger divertor power deposition.

In Fig. 3(b) two C_2 spectra (KME I5) are depicted, where the SP was fixed on plate 2. The first spectrum (L-mode) represents a typical rovibrational population of about 4000 K, whereas the second one (H-mode) shows a significantly lower, unusual population of about 2000 K. The rovibrational population is determined by the plasma parameters and by the break-up mechanism; further investigations are necessary to determine the origin of the population with low temperature. Fig. 3(c) shows the peaked distribution of C_2 and CD light, recorded by KME with fibres I2–I7, around the SP position. The different intensity ratios of C_2 to CD in the two modes provide additional information about the composition of the released particles [5]. These ratios are a factor of 2.6 lower for H-mode, in comparison with discharge #61379, and 3.8 lower for the L-mode at the

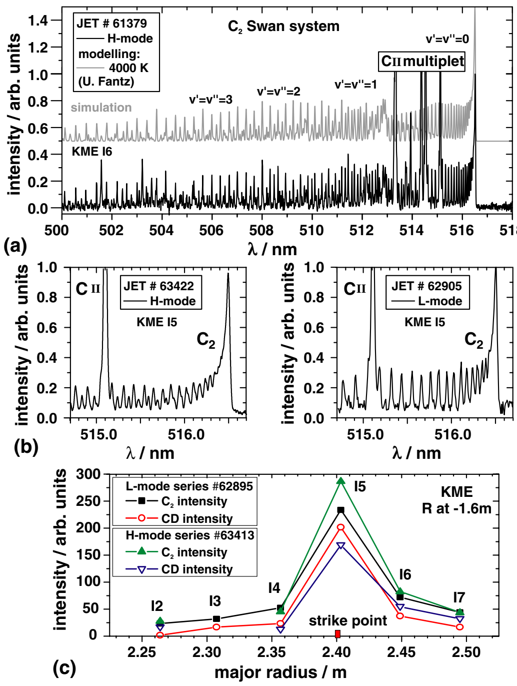

Fig. 3. (a) Measured and simulated spectra of the C_2 Swan band (H-mode, corner configuration). (b) Typical C_2 spectra for an L- and an H-mode discharge with fixed SP on plate 2. (c) C_2 and CD light distribution at the *vt* plates for two series of identical discharges.

location of maximum emission. This underlines the preferred emission of C_2 light according to the preferred release of C_2D_y at the corner, which stepwise dissociates into C_2 as the final molecular product [11].

Carbon sublimation can be ruled out as a source for the C_2 particles. The absence of a black body radiation background, the simultaneous increase of CD and C_2 light and the high rotational temperature of C_2 exclude that the release of carbon clusters is the C_2 particle source [12]. Furthermore, C, C_2 and C_3 are generated by carbon sublimation, but no light emission of C_3 molecules ($A^1\Pi_u \rightarrow X^1\Sigma_g^+$ around 405 nm) was detected.

3.2. Outer divertor

In general, no strong light emission of C_2 and CD has been observed in the outer divertor in L-mode discharges. Dedicated SP sweeps (Fig. 1(a)) through the corner region (#56975–#56980) show no enhanced molecular light emission in ch4 (KS3A), but occasionally thermal radiation [8].

Strong C_2 light emission has been detected in H-mode discharges. In discharge #62564 (17 MW NBI) the SP was positioned at the edge of plate 5 (corner entrance). Fig. 4(a) shows the spectral range around 386 nm, measured by means of KT3A, where the B–X transition of CD and the Deslandres-d'Azambuja transition of C_2 were observed. In Fig. 4(b), the time evolution of the C_2 and CD light are depicted. ϕ_{CD} is almost constant during the entire discharge whereas ϕ_{C_2} varies and has two different phases, although the plasma parameters were nearly constant at the separatrix. ϕ_{C_2} runs through a maximum at the beginning of the discharge ($t = 14.3$ s) and remains nearly constant at about half the maximum value for the later phase. In line with the ϕ_{C_2} increase is the rise of ϕ_{CII}, which might indicate a direct release of C_2 particles. The radial light distribution (Fig. 4(c)) shows a maximum for CD and C_2 in the outermost non-vignetting channel of KT3A, which almost observes the SP position. The maxima, and especially the C_2 one, are more pronounced in the first phase. A quantitative analysis is restricted owing to the vignetting. However, this example shows that at high ion fluxes additional processes and the time evolution of layer properties have to be taken into account.

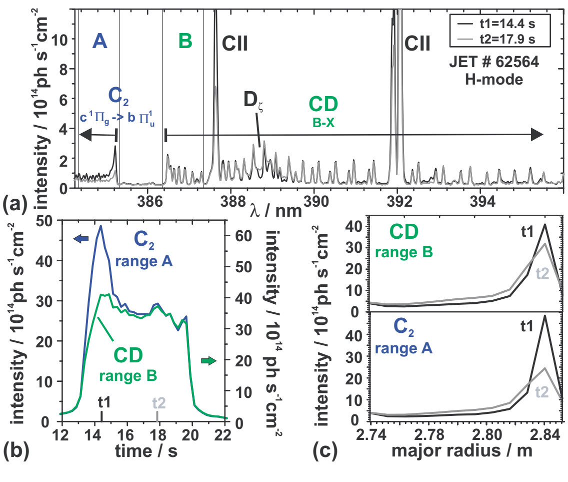

Fig. 4. (a) The CD B–X and the C_2 Deslandres-d'Azambuja band. (b) Time evolution of C_2 (A: 384.4–385.4 nm) and CD (B: 386.4–387.4 nm) in an H-mode discharge and SP on plate 5. (c) Radial distribution of the CD and C_2 intensity.

4. Conclusion

In the present MKII SRP inner divertor, strong C_2 and CD light emission in the corner region has been observed depending on the strike-point position. A reduction of the light emission for successive, identical plasma discharges in L-mode has been measured. According to the C_2/CD photon-flux ratio, the release takes place mainly in the form of C_2D_y. This indicates that the properties of deposited carbon layers are changed by the plasma impact, most probably by thermally and ion-induced release of loosely bound hydrocarbons (soft layer). A release of carbon clusters can be excluded.

We have evidence that in H-mode discharges, where the strike point was fixed at the a-C:H layer location, a complete removal of the layer takes place within one discharge. In the consecutive identical discharges, no enhanced C_2 and CD light could be observed, and further, the ratio of ϕ_{C_2} to ϕ_{CD} drops and then remains constant with a typical value for the horizontal target plate of about 0.3. This underlines that for the analysis the history of previously performed discharges has to be taken into account.

These observations are in agreement with deposition measurements on the QMB, located near the louvre. The strong C_2 and CD light emission is correlated with the decomposition of soft carbon layers and with the massive transport of particles to the louvre. However, the strong light emission cannot always be observed when the strike point touches the corner. Apart from the history effect, hidden parameters like the variations of the layer properties may be important.

In contrast to the inner divertor, strike-point sweeps through the corner of the outer divertor do not show strong C_2 or CD light emission in L-mode discharges. This indicates that a similar soft layer is not present in the view of the detection systems.

References

[1] V. Philipps et al., Plasma Phys. Control. Fusion 45 (12A) (2003) A17.

[2] J.P. Coad et al., J. Nucl. Mater. 313–316 (2003) 419.

[3] G.F. Matthews et al., in: 30th EPS Conference on Control. Fusion and Plasma Phys., St. Petersburg, 7–11 July 2003 ECA Vol. 27A, P-3.198.

[4] A. Pospieszczyk et al., Spectroscopic Studies of Carbon Containing Molecules and their Break-up in Pisces-A (UCLA, Report PPG-1251, 1989).

[5] U. Fantz, in: R.E.H. Clark, D.H. Reiter (Eds.), Nuclear Fusion Research, Springer Series in Chem. Physics Vol. 78, Berlin, 2005.

[6] M.F. Stamp et al., J. Nucl. Mater. 290–293 (2001) 321.

[7] S. Brezinsek et al., Phys. Scr. T 111 (2004) 42.
[8] M.F. Stamp, these Proceedings. doi:10.1016/j.jnucmat.2004.07.061.
[9] A. Huber et al., Phys. Scr. T 111 (2004) 101.
[10] G. Esser, these Proceedings. doi:10.1016/j.jnucmat.2004.10.112.
[11] R. Janev, D. Reiter, Phys. Plasmas 11 (11) (2004) 780.
[12] R.C. Isler et al., Phys. Plasmas 8 (12) (2001) 4417.